JOURNAL OF MATERIALS SCIENCE **35** (2000) 6123–6130

Chemical states of oxygen implanted in SUS 304 stainless steel and pure metals studied by *in situ* XPS using synchrotron radiation

Y. LI
State Key Laboratory of Corrosion and Protection of Metal, Institute of Corrosion and Protection of Metals, ShenYang, 110015, People's Republic of China

Y. BABA, T. SEKIGUCHI
Department of Synchrotron Radiation Research, Japan Atomic Energy Research Institute, Tokai-mura, Naka-gun, Ibaraki-ken, 319-1195, Japan
E-mail: LiYing@icpm.syb.ac.cn

The chemical states of oxygen implanted in SUS304 stainless steel and pure metals (Fe,Ni,Cr) by O_2^+ ion bombardment have been investigated by means of X-ray photoelectron spectroscopy (XPS) using synchrotron soft X-ray. For SUS304, all of implanted oxygen is chemically combined with the constituent metals, forming metallic oxides. For pure metals, on the other hand, only a part of implanted oxygen react with the target metals. The other part of the implanted oxygen in pure metals does not react with the target, and they are inserted into the crystal lattice (we call them as "dissolved oxygen"). The ratio of "dissolved oxygen" to the reacted oxygen depends on the chemical reactivity of target metals.

1. Introduction

Ion-implantation method is widely used for the surface modification of metals such as hardening and corrosion resistance [1–9], because this method is non-equilibrium process and we can produce new layer which can not be obtained by thermal process. Oxygen ion is one of the ideal ions for the improvement of the corrosion resistance of aluminum, magnesium, iron, stainless steel and intermetallic compound [2, 10–16]. In these works, the physical properties such as microstructure and the mechanical properties of the implanted layer have been fully clarified.

Because oxygen is chemically reactive, O^+ ion bombardment on metals would induce various changes of chemical state as well as those of the physical and mechanical properties. However, few research works have been carried out on the chemical state of oxygen implanted in metals. In this present paper, the chemical states of oxygen implanted in SUS304 have been studied by means of *in situ* X-ray photoelectron spectroscopy (XPS). For comparison, the same experiments were carried out for pure metal targets which are components of SUS304 such as iron, chromium and nickel.

2. Experimental methods

2.1. Sample

Commercial type SUS304 stainless steel was provided by the NILACO Co. The chemical composition of SUS304 stainless steel is listed as follow: carbon $<$ 0.0030 at%, silicon $<$ 1.00 at%, manganese $<$ 2.00 at%, phosphorus 0.045 at%, sulfur $<$ 0.030 at%, nickel 8–10.5 at%, chromium 18–20 at%. The other is iron.

The foil of 10 mm $\times$ 10 mm $\times$ 0.5 mm was ground with 400–1000 grit SiC paper, polished with diamond paste of 1.5 μm, washed by distilled water and acetone, and then, kept it in acetone to avoid being oxidized by the oxygen in air. Commercial-type pure metals of iron, chromium and nickel were provided by VACOM Chemical LIT. Company. The purity of the metals is higher than 99.9%. The total size of the specimens were 10 mm $\times$ 10 mm $\times$ 0.5 mm. The sample was polished with $100^{\#}$ SiC paper and washed by distilled water and acetone.

Before the bombardment of O_2^+ ions, the specimen was sputtered with 3-keV Ar^+ ion until a clean surface without any oxide and containment was obtained. Oxygen ions were produced from O_2 source gas. The incident energy of the O_2^+ ion was 3-keV which corresponds to 1.5-keV O^+. The base pressure of system was lower than 2×10^{-9} Torr and the pressure during ion irradiation was kept below 1×10^{-6} Torr. The sample was kept at room temperature during bombardment.

2.2. Analysis method

The measurement system has been described elsewhere [17, 18]. After the oxygen-ion bombardments, the chemical states of oxygen, as well as iron, chromium and nickel, were analyzed by XPS in the same vacuum system as the ion bombardment. The XPS measurement was carried out using synchrotron radiation (SR) as an excitation source, because we can change

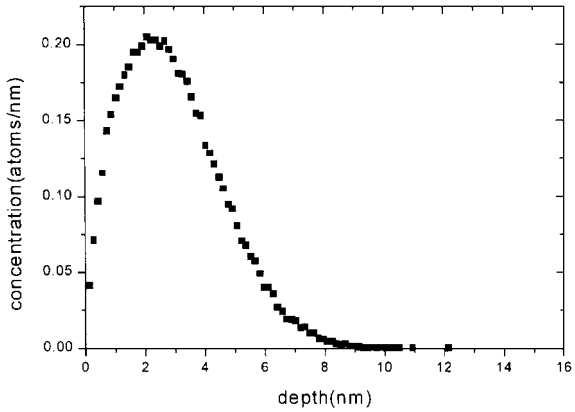

Figure 1 The ion range distribution calculated by TRIM Ion mass: 15.99, Ion angle: 0 degree, Displacement energy for Fe,Cr,Ni: 25 eV.

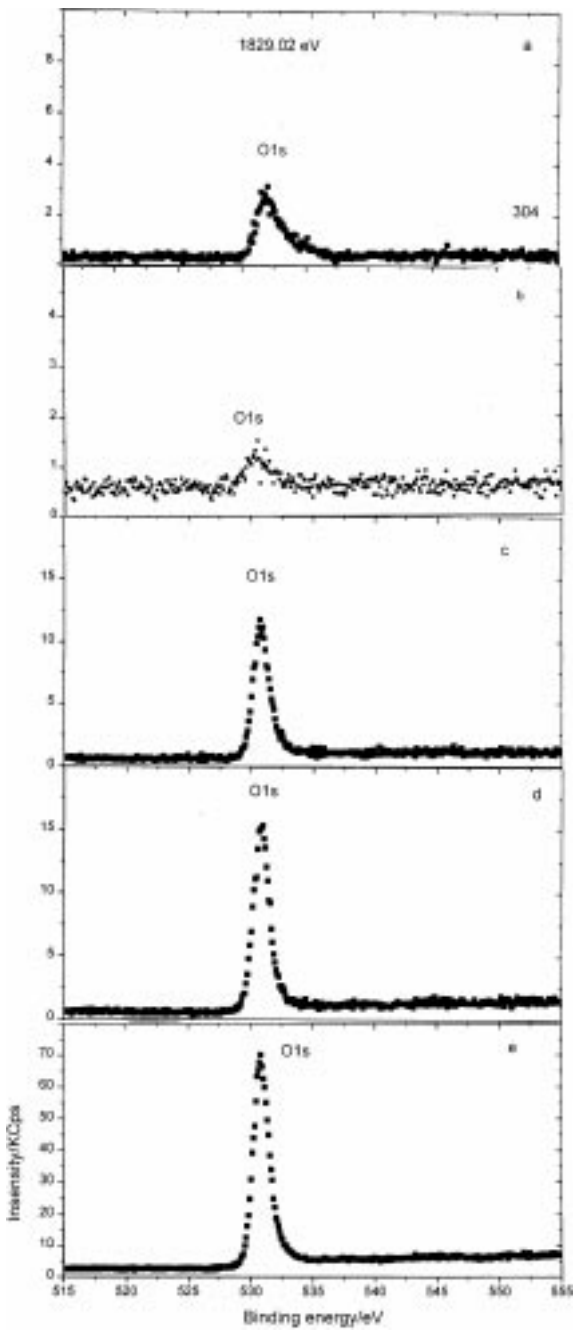

Figure 2 XPS of O1s of SUS304 with different dose of O_2^+ implantation on it. a: without implantation; b: 3.8×10^{15} atoms/cm^2 O_2^+; c: 7.5×10^{15} atoms/cm^2 O_2^+; d: 1.5×10^{16} atoms/cm^2 O_2^+; e: 3.0×10^{16} atoms/cm^2 O_2^+.

the detection depth by changing the incident photon energy. The synchrotron beam line was BL-27 at the Photon Factory in High Energy Accelerator Research Organization (KEK-PF). One of the characteristics of this beam line is that the energy of incident X-ray ranges from 1800 eV–6000 eV, which is wide compared with normal XPS system. Due to the wide energy range of incident X-ray, we can appreciably change the detection depth of XPS analysis. The synchrotron radiation was monochromatized by double crystal monochromator using InSb(111) planes. The energy resolutions of this beam line were 0.9 eV and 1.5 eV at photon energies of 2000 ev and 4000 ev respectively.

The electron energy spectra were obtained using a hemispherical electron analyzer (VSW class-100). The

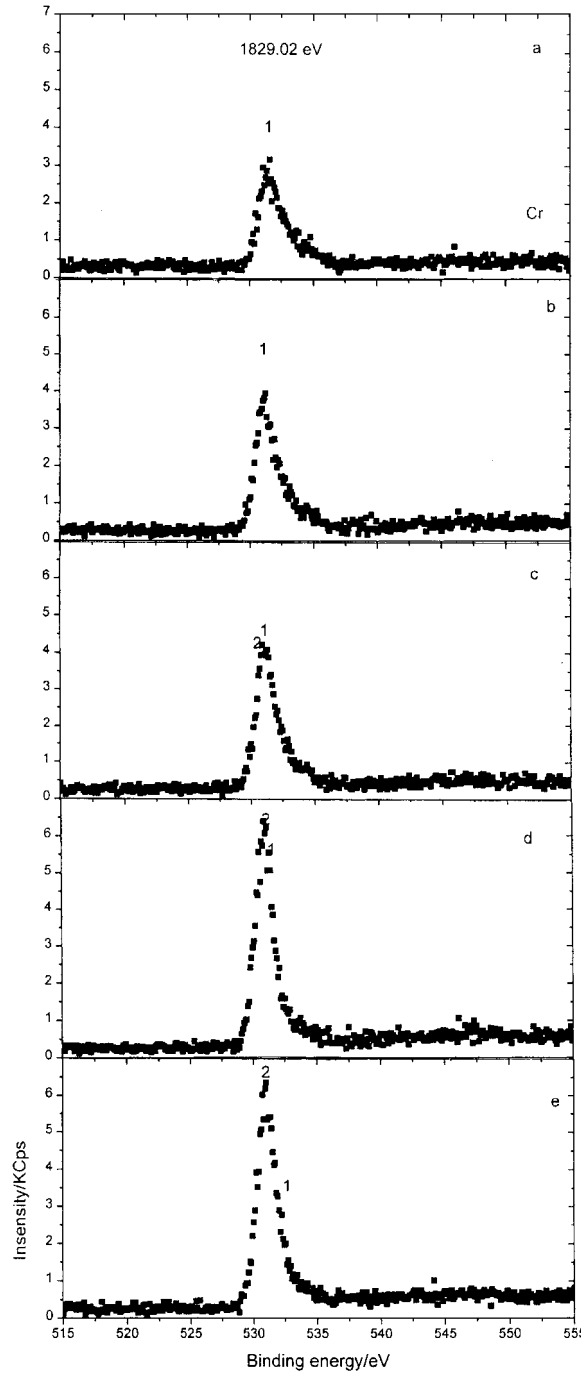

Figure 3 XPS of O1s of pure chromium with different dose of O_2^+ implantation on it. a: without implantation; b: 3.8×10^{15} atoms/cm^2 O_2^+; c: 7.5×10^{15} atoms/cm^2 O_2^+; d: 1.5×10^{16} atoms/cm^2 O_2^+; e: 3.0×10^{16} atoms/cm^2 O_2^+.

sample was irradiated by incident X-ray at an angle of 55 degree and the photoelectron take-off direction was surface normal. The XPS spectra were analyzed with the XPS analysis software provided by VSW Science Instrument LTD. Peak location, width at half the height and peak area were provided after curve fitting.

3. Results and discussion

The depth distribution of oxygen implanted in SUS304 can be calculated by the Trim (The Transport of Ion in Matter)95 software basing on the original work by J. P. Biersack on range of algorithms [19] and J. F. Ziegler on stopping theory [20]. The result is shown in Fig. 1. The average range is 2.9 nm for the 1.5 keV O^+ ion in SUS304 and the maximum concentration of oxygen is located around 2.0 nm. Taking account of that result and the binding energy of O1s, we tuned the energy of the incident X-ray at 1829.24 eV, because the electron inelastic mean free paths (IMFP) of the O1s photoelectron at this photon energy is 2.01 nm which is close to the calculated maximum concentration of oxygen.

The XPS spectra of O1s line for SUS304 and pure metals after bombardment of O_2^+ ions at various fluences are shown in Figs 2–5. The XPS spectra of Fe2p,Ni2p and Cr2p for SUS304 and pure metals after

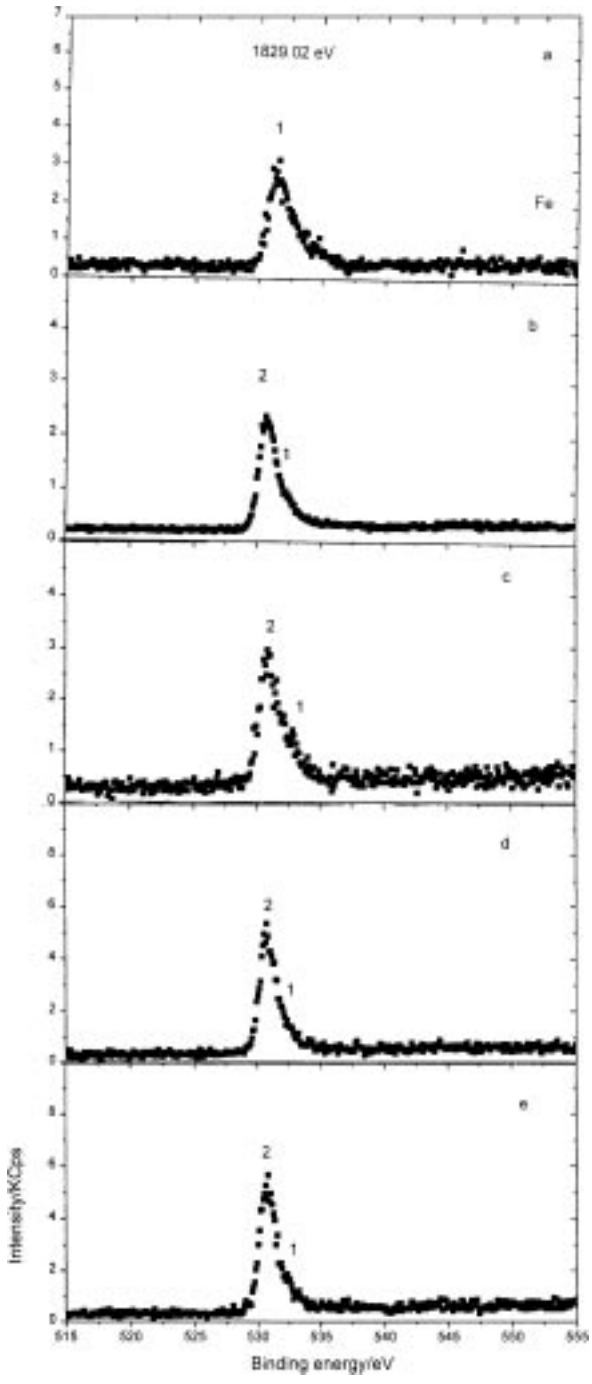

Figure 4 XPS of O1s of pure iron with different dose of O_2^+ implantation on it. a: without implantation; b: 3.8×10^{15} atoms/cm^2 O_2^+; c: 7.5×10^{15} atoms/cm^2 O_2^+; d: 1.5×10^{16} atoms/cm^2 O_2^+; e: 3.0×10^{16} atoms/cm^2 O_2^+.

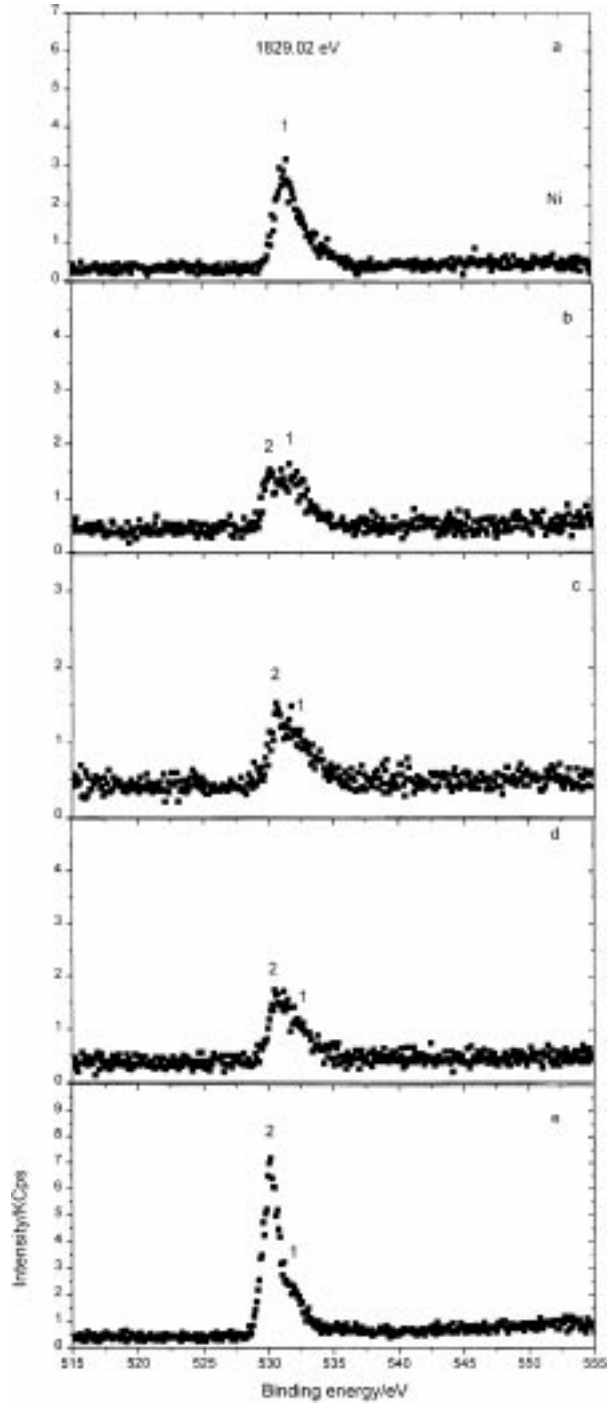

Figure 5 XPS of O1s of pure nickel with different dose of O_2^+ implantation on it. a: without implantation; b: 3.8×10^{15} atoms/cm^2 O_2^+; c: 7.5×10^{15} atoms/cm^2 O_2^+; d: 1.5×10^{16} atoms/cm^2 O_2^+; e: 3.0×10^{16} atoms/cm^2 O_2^+.

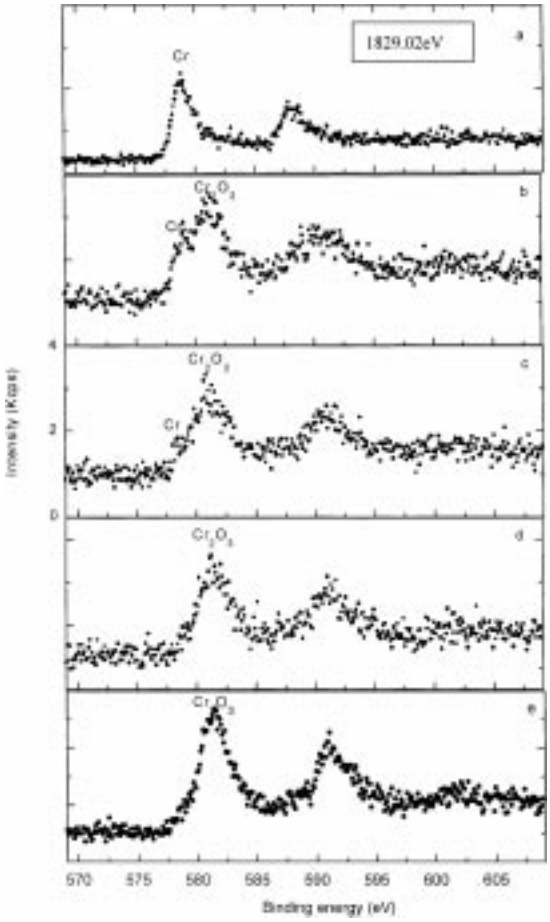

(A)

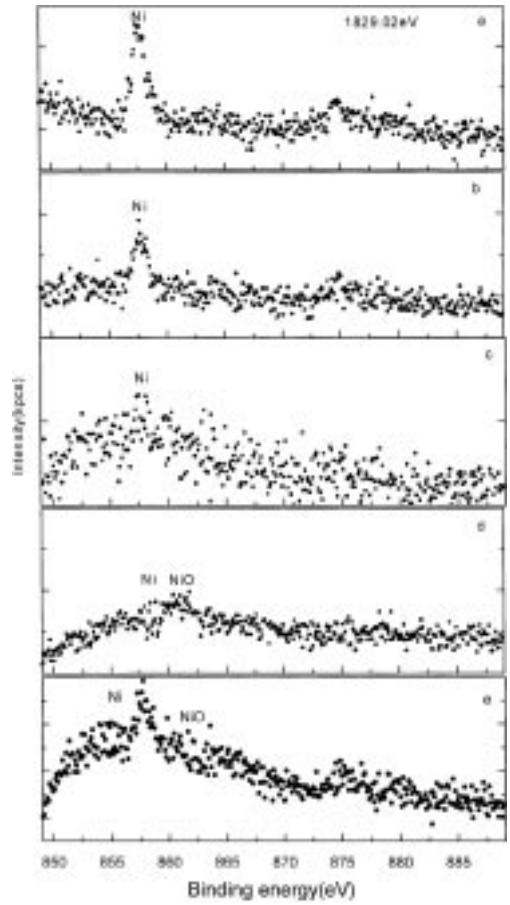

(B)

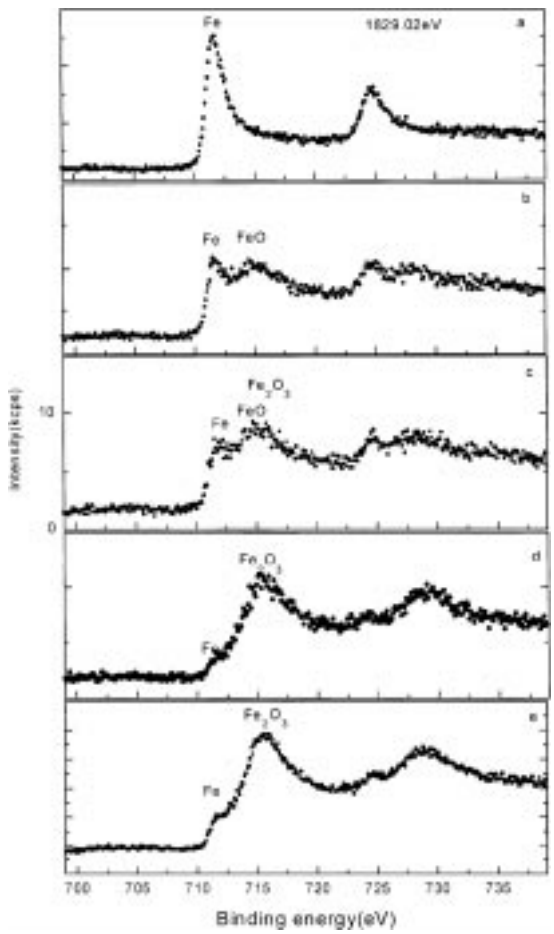

(C)

Figure 6 XPS spectra of (A) Cr2p, (B) Ni2p, (C) Fe2p in SUS304 stainless steel before and after implantation of O_2^+. a: without implantation; b: 3.75×10^{15} atoms/cm^2 O_2^+; c: 7.5×10^{15} atoms/cm^2 O_2^+; d: 1.5×10^{16} atoms/cm^2 O_2^+; e: 3.0×10^{16} atoms/cm^2 O_2^+.

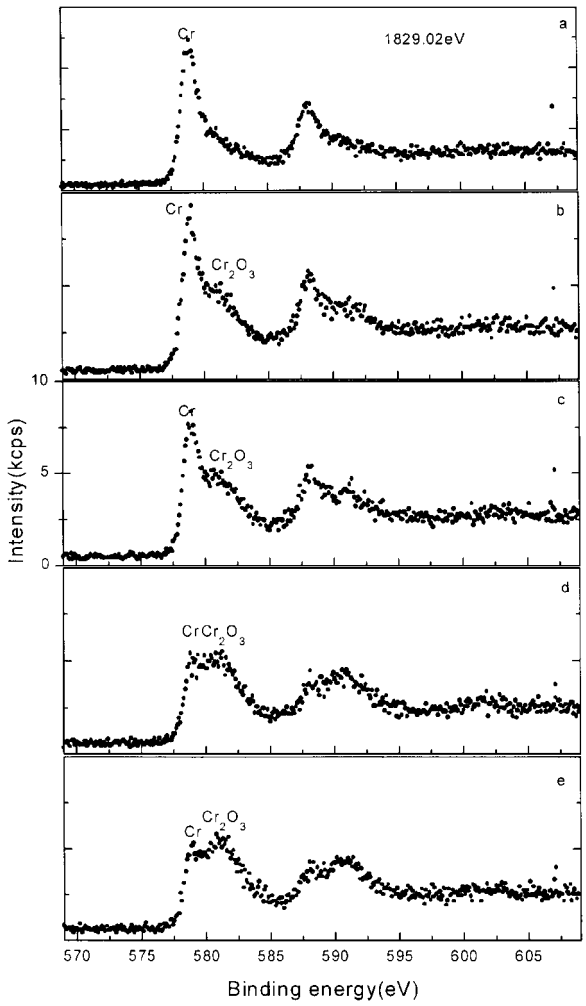

(A)

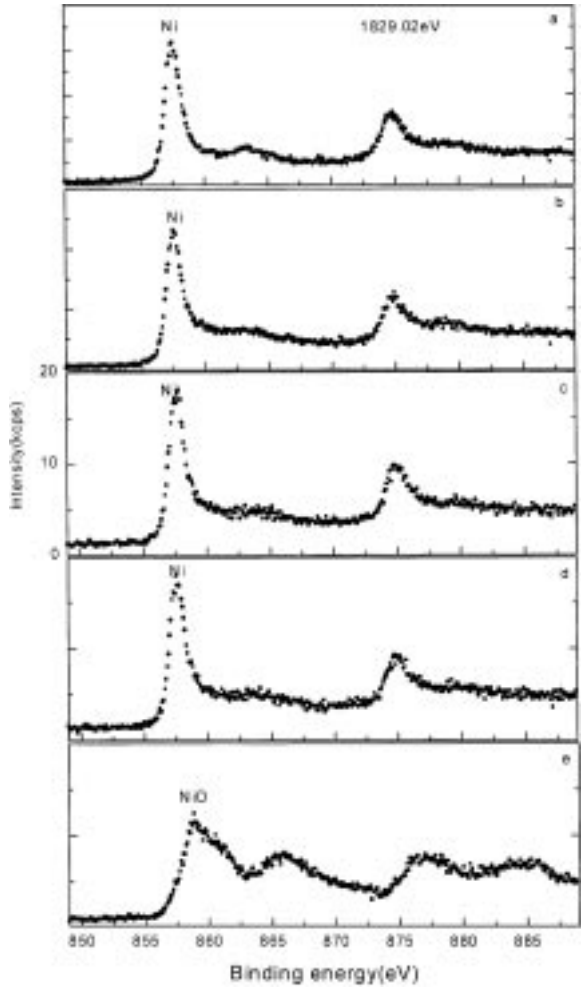

(B)

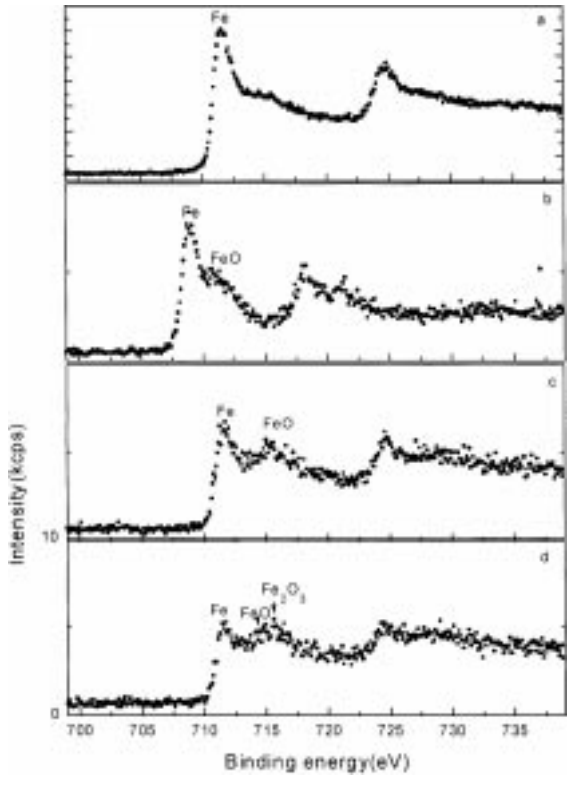

(C)

Figure 7 XPS spectra of (A) Cr2p, (B) Ni2p, (C) Fe2p in pure Cr before and after implantation of O_2^+. a: without implantation; b: 3.75×10^{15} atoms/cm^2 O_2^+; c: 7.5×10^{15} atoms/cm^2 O_2^+; d: 1.5×10^{16} atoms/cm^2 O_2^+; e: 3.0×10^{16} atoms/cm^2 O_2^+.

bombardment of O_2^+ ions at various fluence are shown in Figs 6 and 7. It is clearly observed that the peak position of the O1s line for SUS304 is constant regardless of the fluence. On the other hand, the O1s line for pure iron, chromium and nickel have double structure for all fluences. It suggests that there are two chemical states for oxygen in pure metals in contrast to those in SUS304.

The relative concentration of oxygen in SUS304 and pure metals can be calculated by the following equation,

$$I = nK\lambda\sigma \tag{1}$$

where I is the intensity of photoelectron, n the number of atomic per unit volume, K a parameter decided by the characters of instrument and beam line, σ photoionization cross section and λ the electron inelastic mean free paths (IMFP). The value of σ and λ change with the electron kinetic energy. The value of IMFP in Fe,Cr,Ni at different electron energy have been calculated based on the work by Tanuma *et al.* [21] and Powell [22]. The value of σ of Fe2p3/2, Cr 2p3/2, Ni 2p3/2 and O 1s has been estimated by the Scofield's calculation [23]. The value of λ and σ of each elements is listed in Table I.

Based on the formula (1), the relative concentration of oxygen (C_{ox}) in the metal matrix can be calculated as follows:

$$C_{ox} = \left(\frac{I_{O1s}}{\sigma_{01s}\lambda_{01s}}\right) \div \left[\frac{I_{Fe2p3/2}}{(\sigma_{Fe2p3/2}\lambda_{Fep3/2})} + \frac{I_{Cr2p3/2}}{(\sigma_{Cr2p3/2}\lambda_{Cr2p3/2})} + \frac{I_{Ni2p3/2}}{(\sigma_{Ni2p3/2}\lambda_{Nip3/2})} + \frac{I_{O1s}}{(\sigma_{01s}\lambda_{01s})}\right] \tag{2}$$

TABLE I The parameter of σ and λ for Fe,Cr,Ni,O

	O1s	$Fe2p_{3/2}$	$Cr2p_{3/2}$	$Ni2p_{3/2}$
Photon energy (eV)	1829.02	1829.02	1829.02	1829.02
Kinetic energy (eV)	1294.2	1117.3	1250.2	971.3
λ (angstrom)	21.0	20.8	18.4	18.0
σ (barn) 10^4	2.82	7.23	10.38	14.11

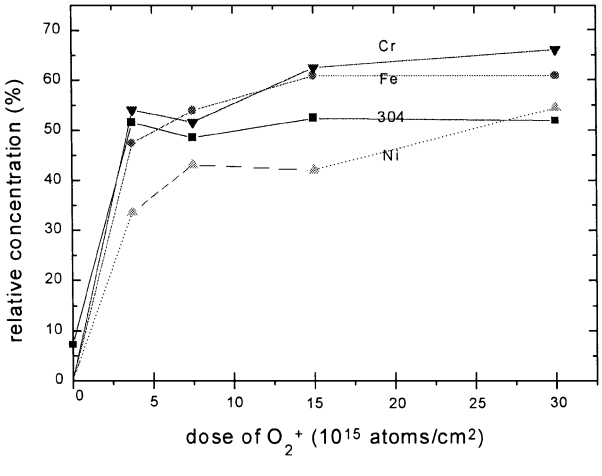

Figure 8 The relative concentration of oxygen in SUS304 and pure metals oxide layer during implantation.

where the elements and orbitals to be concerned are indicated as suffixes. The relative concentration of oxygen in SUS304 and pure metal oxide layer are shown in Fig. 8 as a function of fluence of oxygen ions. At low fluence region below 5×10^{15} atoms/cm^2, the concentration of oxygen increases sharply with the O^+ fluence, but it saturates at high fluence region over 10^{16} atoms/cm^2.

Concerning the chemical state of oxygen atom in the metal lattice, there are two possibilities. The first is the oxygen occupied the vacancy in the lattice or just inserted in the interstitial site. Here we will call this oxygen as dissolved oxygen. In this case, there exist no chemical interaction between oxygen and metal. The second is the oxygen reacted with the metal, forming metallic oxide. We call them as the "reacted oxygen". The concentration of total oxygen atoms ("dissolved oxygen" and "reacted oxygen") can be calculated according to the total area of the O1s peak. The "reacted oxygen" atoms can be specified according to the chemical shift of the metal 2p XPS peak due to the oxide formation. Therefore, the relative concentration of the total oxygen and the "reacted oxygen" can be calculated by those two kinds of XPS peak. The results are shown in Fig. 9.

From Fig. 9 it can be seen that the concentration of oxygen in SUS304 calculated by the two kinds of XPS peak area is the same. That means that all of the oxygen atoms reacted with the metal atoms. On the other hand, the concentration of oxygen in pure metals calculated by the two kinds of XPS peak area were not the same (see Fig. 9). Only a part of oxygen atoms reacted with metal atoms.

From Figs 3–5, it can be seen that the O1s peaks in pure metal targets have double structures. The peaks are located at 531.6 eV and 530.8 eV. It can be confirmed that 531.6 eV peak is originated from the reacted oxygen for its high binding energy. The 530.8 eV peak is attributed to the dissolved oxygen.

The fluence dependence of the relative concentrations of two kinds of oxygen atoms in pure metals is shown in Fig. 10. For pure chromium target, the concentration of "reacted oxygen" is always higher than that of "dissolved oxygen", but the ratio of two kinds of oxygen does not change regardless the fluence. For pure iron, before Fe_2O_3 produced, the behavior of O^+ ion implantation is similar to that of pure chromium. However, the concentration of the dissolved oxygen increases when Fe_2O_3 is produced. The oxide reaction is difficult to take place when Fe_2O_3 is formed. For pure nickel target, the concentration of dissolved oxygen increased sharply at low fluence region, but it decreased when NiO produced. The results indicated that the substitution of the vacancy in the lattice or interstitial site by the oxygen atom is the first step in implantation process in pure nickel, then, these dissolved oxygen are converted to NiO when enough O^+ ion is implanted in the target. From those results, it can be concluded that SUS304 stainless steel has the highest reactivity with the O^+ ion, pure nickel is the lowest in reverse.

As well known, once oxygen is implanted in the structure, it need to react to form chemical band, Since the implanted species is O^+ ion, which will probably be

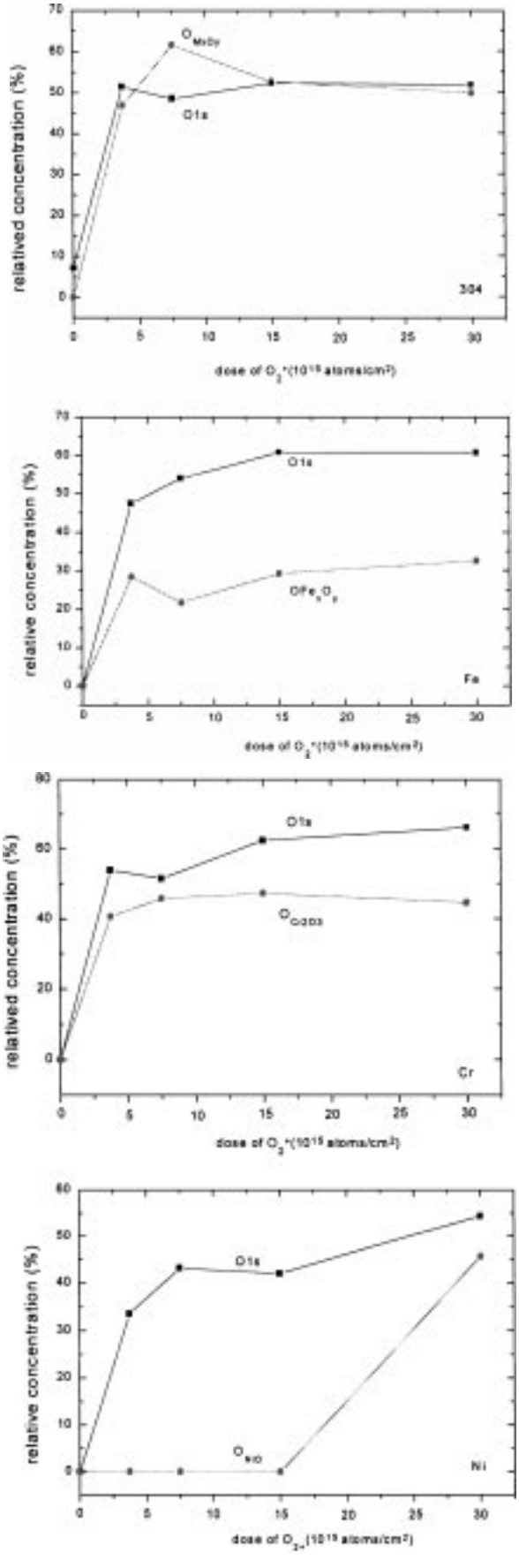

Figure 9 The relative concentration of total implanted oxygen and "reacted oxygen" on SUS304 and pure metals during implantation.

neutralized at or near surface. Then, the further chemical reaction between oxygen atom and target atom will take place if the atoms have enough energy. From XPS spectra of metals on SUS304 and pure metals (see Figs 6

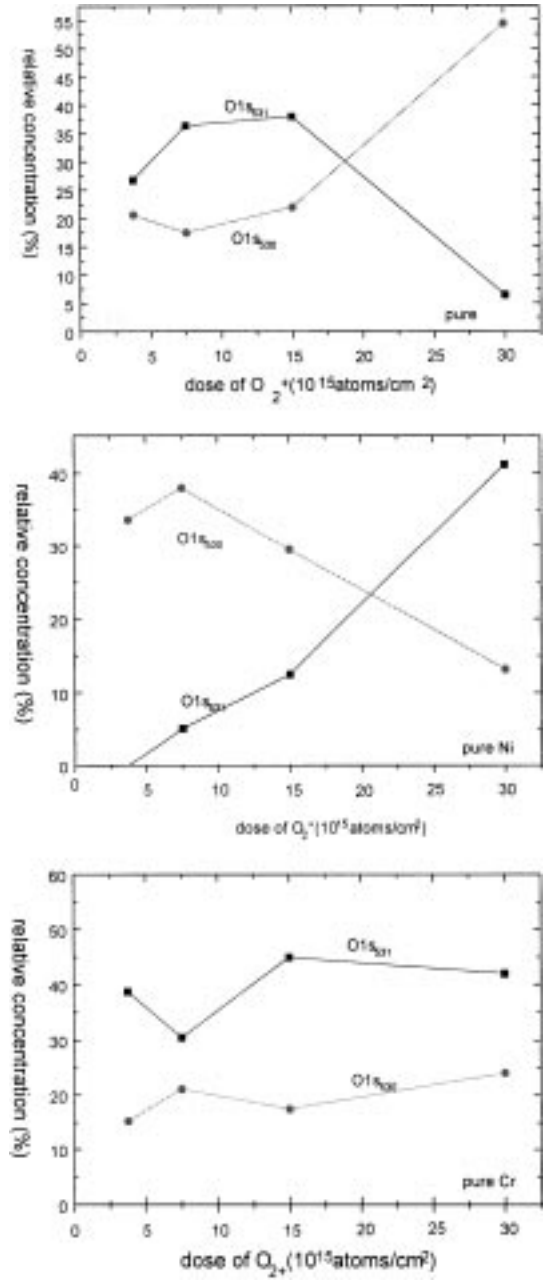

Figure 10 The percentage of chemical state O1s at 530 eV and 01s at 531 eV on pure metal.

and 7), it can be seen that the further oxide reaction took place on each metal targets after large amount of O^+ ion implanted. The reaction are described as follows:

$$O + 2e \rightarrow O^{2-}$$

$$Ni \rightarrow Ni^{2+} + 2e \quad \text{(for pure Ni target)}$$

$$Cr \rightarrow Cr^{3+} + 3e \quad \text{(for pure Cr target)}$$

$$Fe \rightarrow Fe^{2+} + 2e \quad \text{and}$$

$$Fe^{2+} \rightarrow Fe^{3+} + e \quad \text{(for pure Fe target)}$$

For SUS304, all of reactions above took place. In this case, all the reaction is predominated by the property of targets because of the same energy of the implanted O^+ ion. The chemical reactivity and the mobility of the target atoms play a big role in the implantation process. For the same element, the oxide reaction will take place easier if the target atoms have higher mobility. In this

case, the dissolved oxygen concentration is lower in the target. As well known, the target atoms will be set in motion in the cascade with the energies above their displacement energy. The displacement energy for Cr, Ni (crystal) and Fe (crystal) are 28 eV, 33 eV and 44 eV respectively [24]. That means Cr is easiest to move in the SUS304 target than the others metal atoms and will play a big role during implantation. Furthermore, compared to pure metals, there are many defects in SUS304 stainless steel. It is very easy for interstitial to move along the defect, therefore, Cr atom is easier to move in SUS304 than in pure Cr. The oxide reaction between Cr and oxygen is easier to take place in stainless steel. That is the reason why there is no dissolved oxygen in SUS304. For pure Fe, the mobility of FeO is lower than Fe, therefore, the oxide reaction is hold back as the FeO formed, the dissolved oxygen concentration increased in this case. For pure Ni, the chemical reactivity and the mobility of the Ni are not high enough. There is also some dissolved oxygen even through large amount of O^+ ion implanted in it.

4. Summary

The chemical states of oxygen implanted in SUS304 stainless steel and pure metals have been investigated by *in-situ* SR-XPS. For SUS304, all of the implanted oxygen chemically combined with the metals forming metallic oxides. For pure metal targets, on the other hand, there are two chemical states of oxygen in the lattice. One is the dissolved oxygen occupied the vacancy in the crystal lattice or inserted into the crystal lattice. The other is the reacted oxygen that chemically combined with metals forming metallic oxide. The ratio of these two kinds of oxygen is different among the target metals. For iron, the chemical reaction was hold back when Fe_2O_3 is produced. On the other hand, dissolved oxygen is predominant at the first step in pure nickel, then once NiO lattice is formed, these dissolved oxygen are converted to NiO. The oxide reaction takes place easily if the target atom has high mobility and reactivity.

It is easiest for Cr atom to move in SUS304 for the many defects existed in SUS304 and also for higher mobility Cr has. The oxide reaction is easier to take place in SUS304. That is the reason why there is no dissolved oxygen existed in SUS304.

Acknowledgments

The authors are pleased to thank the staff of the photon Factory in the High Energy Accelerator Research Organization for their support through the XPS measurement. This work was supported by JAERI under STA Scientist Exchange Program. One of the authors (Y.L) also expresses her deepest gratitude to STA and JAERI. This work is also subsidized with the Special Funds for the Major State Basic Research Projects G19990650.

References

1. ELECTROTECHNICAL LAB, *Bulletin of the Electrotechical Laboratory* **57** (1993) 4.
2. T. FUJIHANA and M. IWAKI, *Surf. Coat. Technol.* **66** (199) 1.
3. S. TANIGUCHI, *Werkstoffe und Korrosion* **48** (1997) 1.
4. F. H STOTT Z. PEIDE, W. A. GRANT and R. P. M. PROCIER, *Corrosion Science* **22** (1982) 305.
5. M. J. BENNETT and S. J. BULL, *Werkstoffe und Korrosion* **48** (1997) 48.
6. K. TAKAHASHI, M. NIKOLOVA and M. IWAKI, *J. Appl. Electrochem.* **24** (1994) 52.
7. C. J. MCHARGUE, M. B. LEWIS, J. M. WILLIAMS and B. R. APPLETON, *Mater. Sci.* **69** (1985) 391.
8. D P/S V. VOLLMER, J. D. GARBER, G. A. GLASS, R. D. BRAUN, T. J. ST. JOHN and W-J. SHEU, *Corrosion Science.* **40** (1998) 297.
9. R. G. MUSKET, UCRL-98998, CONF-881151-28.
10. A. MITSUO, S. TANAKA and T. TANAKI, Report of the Tokyo Metropolitan Industrial Technology Center, No. 27, 1998, p. 17.
11. M. SCHENEIDER, K. NOCKE and E. RICHTER, *Galvanotechnik* **89** (1998) 2524.
12. M. SCHENEIDER and K. NOCKE, Netherlands Society for Material Science, 1997, p. 305.
13. D. J. REJ, N. V. GAVRILOV and D. EMLIN, Report:LA-UR-95-4148, CONF-951155-71, Department of Energy, Washington DC, 1995, p. 7.
14. J. M. SAXTON, I. C. LYON, E. CHATZITHEODOREDIS, J. D. GILMOUR and G. TURNER, National Aeronautics and Space Administration, Washington. DC, Jun 1992, p. 1.
15. D. KRUPA, J. BASZKIEWICZ, J. KOZUBOWSKI, A. BARCZ, G. GAWLIK, J. JADIELSKI and B. LARISCH, *Surface Coating Technology* **96** (1997) 223.
16. R. J. HANRAHAN JR., E. D. VERINK JR., E. O. RISTOLAINEN and S. P. WITHROW, The Minerals, Metals and Materials Society, Warrendale, PA, 1994, p. 643.
17. H. YAMAMOTO, Y. BABA and T. A. SASAKI, *J. Surf. Sci. Soc. Jpn.* **13** (1992) 310.
18. *Idem., Nucl. Instrum. Methods Phys. Res. B* **73** (1993) 587.
19. J. P. BIERSACK and L. HAGGMARK, *Nucl. Instr. and Meth.* **174** (1980) 257.
20. J. F. ZIEGLER, "The Stopping and Range of Ions in Matter, Vols. 2–6" (Pergamom Press, 1977–1985).
21. S. TANUMA, C. J. POWELL and D. R. PENM, *Surface and Interface Analysis* **17** (1990) 911.
22. C. J. POWELL, *Surface Science* **44** (1974) 29.
23. J. M. SCOFIELD, *UCRL-51326* (1973).
24. E. BALANZAT and S. BOUFFARD, *Solid State Phenomena* **30&31** (1993) 7.

Received 13 September 1999
and accepted 2 May 2000